

Dual Band RF Harvesting with Low-Cost Lossy Substrate for Low-Power Supply System

Spyridon-Nektarios Daskalakis¹, Apostolos Georgiadis², Aggelos Bletsas³, Christos Kalialakis⁴

¹Technical University of Crete, Greece, sdaskalakis@isc.tuc.gr

²Centre Tecnologic de Telecomunicacions de Catalunya, Spain, ageorgiadis@cttc.es

³Technical University of Crete, Greece, aggelos@telecom.tuc.gr

⁴Centre Tecnologic de Telecomunicacions de Catalunya, Spain, christos.kalialakis@cttc.es

Abstract—A high efficiency, low-complexity, low-cost rectifier for low-power density and low-power input is analyzed, fabricated and measured. The design consists of a double diode rectifier with operation in the two frequency bands of 900 MHz ISM and FM, simultaneously. Although the design uses a low-cost, lossy FR-4 substrate and a low-complexity rectifier circuit, the RF-to-DC rectification efficiency achieves 14.49% and 27.44% at 868 MHz and 97.5 MHz, respectively, for input power of -20 dBm. Measurement results agree with simulations. The rectifier was connected to a commercial boost converter in order to manage and improve the output power of the rectifier. The end-to-end efficiency of the system was calculated to 21% for input power of -15 dBm and frequency of 97.5 MHz, despite the use of a low-cost, lossy substrate.

Index Terms—Energy harvesting, rectifiers, boost converters.

I. INTRODUCTION

All over the world, the number of radio frequency (RF) emitters has been continuously increasing, due to widespread deployment of wireless technologies, such as cellular networks, Wi-Fi, digital TV and wireless sensor networks (WSN). Collection of ambient RF energy and its use of powering electrical devices is an engineering challenge [1]. Over the last years, wireless power transfer (WPT) based on far-field electromagnetic radiation is recommended for large amount of sensors due to their necessity to be autonomous and self-sustained in power [2], while battery replacement is a lengthy and costly procedure in large sensor networks. This WPT concept is suitable for Internet of Things (IoT) applications such as environmental WSNs and sensor networks for smart cities. The collection of unused ambient RF energy with rectifiers and supply of backscatter radio WSNs [3], [4] for example, is a great engineering challenge. In this work, FM and VHF-UHF carrier emitters (e.g., in bistatic scatter radio sensor networks [5], [6]) will be considered as potential RF power sources. On the other hand, ambient RF energy harvesting offers a relatively low energy density of some $\mu W/cm^2$, compared to other power sources (e.g. solar energy or energy from soil [7]), however it can operate in hybrid mode, in conjunction with multiple other sources [8]. Efficiency is an important parameter in a rectifier topology, i.e. the ratio of DC output power to RF input power. Nowadays, significant research effort has been directed towards high-efficiency rectifiers. Many attempts emphasize on the required impedance matching circuit inductances, while minimizing reflection coefficient.

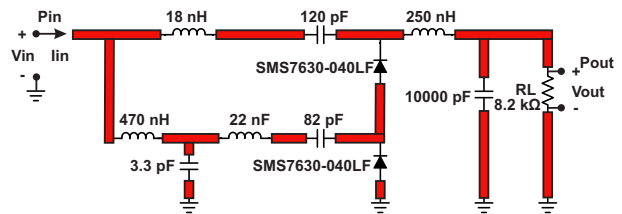


Fig. 1. The double diode rectifier design.

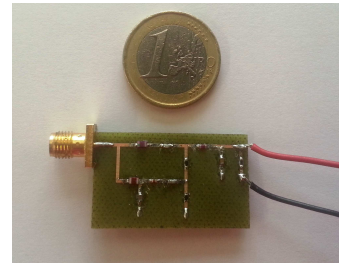


Fig. 2. The fabricated top layer of the rectifier.

For example, RF-to-DC rectification efficiency of 20.5% and 35.3% was attained in [9] for -20 dBm and -10 dBm input power, respectively. This work is summarized as follows: in Section II, a rectifier circuit is presented. In Section III, a dual band printed antenna is described. In Section IV, the use of a commercial DC-DC converter is described and the overall end-to-end efficiency is derived. Work is concluded in Section V.

II. RECTIFIER

A. Rectifier Design and Analysis

In this work, an efficient low-cost and low-complexity rectifier is developed for low-power input. The rectifier is based on double rectification circuit with single diodes as depicted in Fig. 1. The RF input power is converted to DC power through the low-cost Schottky diodes (SMS7630-040LF). The matching circuit (inductors combined with capacitors) reduces the reflection losses of the incoming wave, while the rectifier was designed to operate at 868 MHz (UHF ISM frequency in Europe) and at 97.5 MHz (center of FM band), simultaneously. Harmonic-balance and Momentum solver was employed for simulations. The FR-4 substrate was modelled with $\epsilon_r = 4.4$,

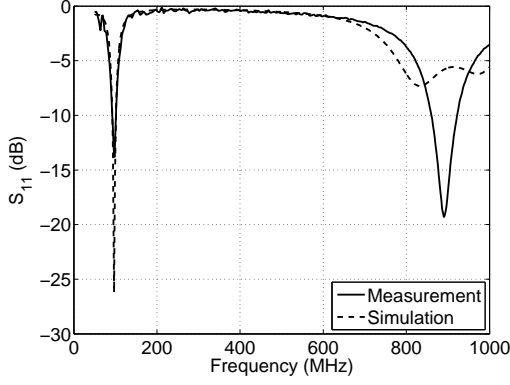


Fig. 3. Reflection coefficient at the input of rectifier.

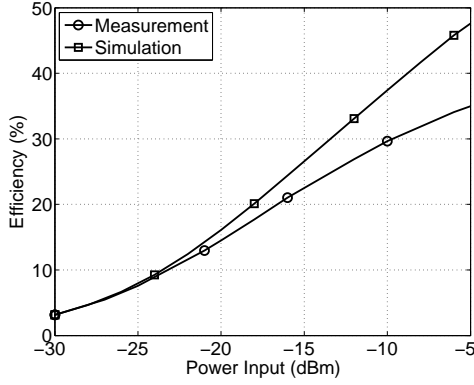


Fig. 4. Rectifier efficiency versus total power input at 868 MHz.

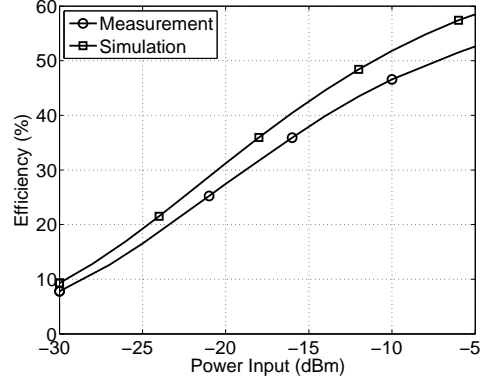


Fig. 5. Rectifier efficiency versus total power input at 97.5 MHz.

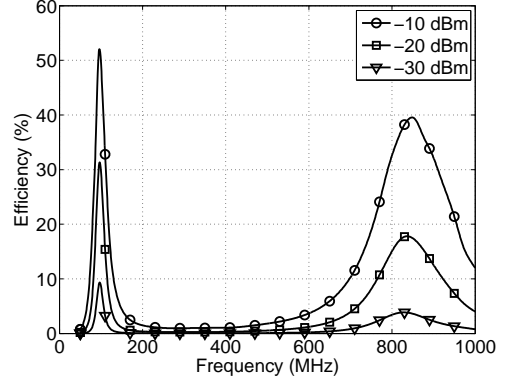


Fig. 6. Rectifier efficiency versus frequency for different power inputs.

$\tan \delta = 0.025$, copper thickness $35 \mu\text{m}$ and substrate height 1.6 mm . The first goal of modelling and simulation was the maximization of the RF to DC efficiency:

$$\eta = \frac{P_{\text{out}}}{P_{\text{in}}} = \frac{V_{\text{out}}^2/R_L}{P_{\text{in}}}, \quad (1)$$

with P_{in} , P_{out} the input and output power and V_{out} the voltage across the load R_L . The second goal was the minimization of reflection coefficient,

$$\Gamma_{\text{in}} = \frac{Z_{\text{in}} - 50}{Z_{\text{in}} + 50}, \quad (2)$$

for input power $P_{\text{in}} -20 \text{ dBm}$ at 868 MHz and 97.5 MHz . The input impedance Z_{in} is defined as (Fig. 1):

$$Z_{\text{in}} = \frac{V_{\text{in}}}{I_{\text{in}}}. \quad (3)$$

After optimization, the dual-band prototype was implemented with discrete components and fixed trace dimensions, as shown in Fig. 2. The load at the output (R_L) was fixed at $9.2 \text{ k}\Omega$. Measurements were employed after that, using a signal generator and a voltmeter. The simulated and measured reflection coefficient S_{11} is depicted in Fig. 3. Reasonable agreement between predicted and measured results is observed at both frequency bands. Figs. 4 and 5 depict efficiency η

versus P_{in} for measurement and simulated results for the two separate bands. According to measured results, the efficiency is 14.49% and 27.44% at 868 MHz and 97.5 MHz , respectively for $P_{\text{in}} = -20 \text{ dBm}$. For $P_{\text{in}} = -10 \text{ dBm}$ the results are 29.64% and 46.58% for 868 MHz and 97.5 MHz , respectively.

The simulated efficiency versus frequency for three power input levels is depicted in Fig. 6. As expected, the rectifier operates optimally at 868 MHz and 97.5 MHz . Figs. 7 and 8 show the relationship between rectifier efficiency and load. Frequency is now fixed at 868 MHz for Fig. 7 and at 97.5 MHz for Fig. 8. It is observed that the $9.2 \text{ k}\Omega$ load is appropriate for 868 MHz but not for 97.5 MHz . Finally, Fig. 9 offers the measured open circuit voltage (without load) versus input power, for the two frequency bands. As expected, the relationship is not linear due to the non linearity of the discrete components.

III. ANTENNA DESIGN

In order to supply the rectifier with wirelessly harvested power, a microstrip multi-band antenna was designed and fabricated. Specifically, a hybrid microstrip monopole antenna was designed to operate at ISM band (around 868 MHz) and at FM band (around 100 MHz). The design is a variation of a monopole antenna (of wide-band operation) with a loop for

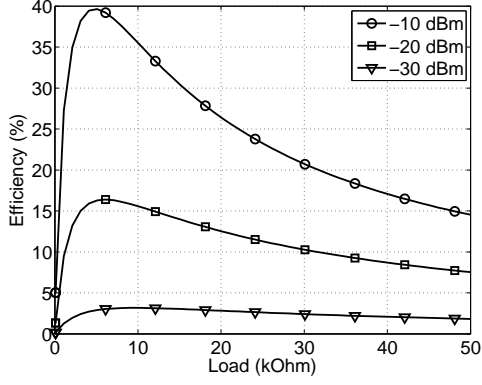


Fig. 7. Rectifier efficiency for 868 MHz versus load for different power inputs.

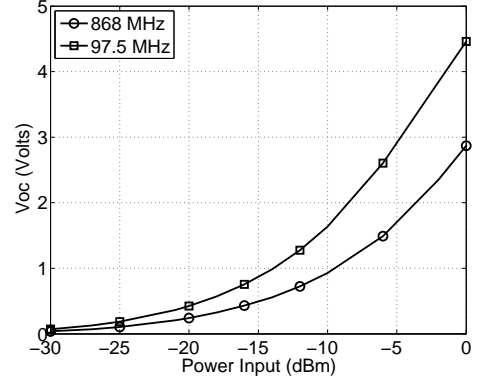


Fig. 9. Measured rectifier output open circuit voltage for 97.5 MHz and 868 MHz.

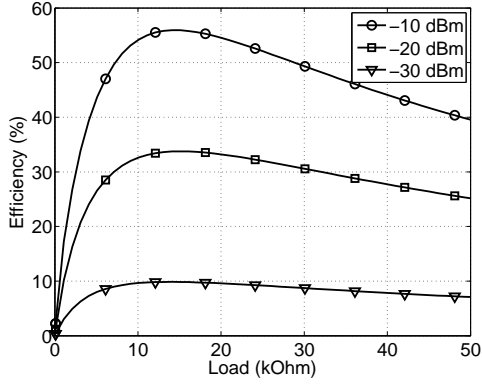


Fig. 8. Rectifier efficiency for 97.5 MHz versus load for different power inputs.

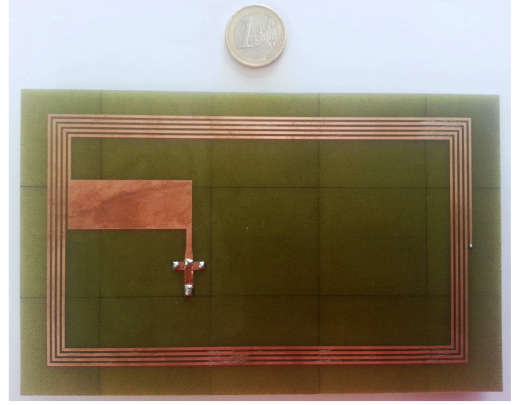


Fig. 10. The fabricated multi-band antenna.

FM band resonance (and low fabrication complexity) on FR4 substrate. The fabricated antenna is depicted in Fig. 10 and its measured reflection coefficient is depicted in Fig. 11.

IV. BOOST CONVERTER

Texas Instrument BQ25504 [10] was chosen as low-power DC-DC converter. The boost converter was combined with two external MOSFET switches (Fig. 12). One PMOS between load (LED) and V_{BAT} and one NMOS for the inverted V_{BAT_OK} signal. The converter is an integrated-circuit with maximum power point tracking (MPPT), minimum cold start voltage and typical input power of 330 mV and 10 uW, respectively. It has also ultra low-power input power levels with low quiescent current (330 nA). It is programmed by resistors and continuously charges a 100 uF storage capacitor (C_s). A LED with maximum current consumption at 20 mA (emulating the energy consuming circuit such as a sensor) was automatically connected through the PMOS switch to the capacitor, when the capacitor increasing voltage reached an upper limit $V_{high} = 2.82$ V and was automatically disconnected, when the capacitor decreasing voltage reached a lower limit $V_{low} = 1.63$ V. When the minimum voltage V_{low} is reached, the boost converter and MPPT start to operate and a charge-

discharge cycle at the load begins, causing the LED to flash. The charge-discharge operation of the LED can be observed in Fig. 14 from the boosted signal V_{BAT} . Using the converter topology of Fig. 13 and a DAQ for capturing the signals, we exported the rectifier output voltage V_{IN_DC} and the boost converter output V_{BAT} voltage for 800 seconds. The rectifier P_{in} was -15 dBm at 97.5 MHz. Finally, it is noted that the boost converter was self-started and no external energy was used.

A. End-to-End Efficiency

The duty cycle of the LED can be used to calculate the efficiency of the system and according to [11], the total end-to-end efficiency of the whole system is:

$$\eta_{total} = \frac{E_{DC}}{E_{in}} = \frac{C_s \frac{V_{high}^2 - V_{low}^2}{2}}{\int_0^{t_{cycle}} P_{in} dt}. \quad (4)$$

E_{DC} is the output DC energy and E_{in} the rectifier output energy. E_{in} can be calculated by integrating the time averaged P_{in} over a cycle time t_{cycle} . The cycle time is the charge-discharge time of the storage capacitor between V_{high} and V_{low} . From measurements of Fig. 14, E_{DC} was calculated at

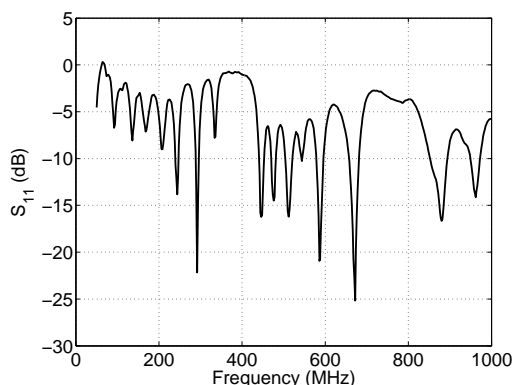


Fig. 11. Reflection coefficient of the multi-band antenna.

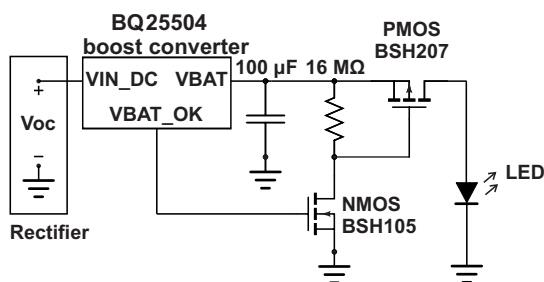


Fig. 12. Boost converter schematic with the low-power BQ25504.

265.17 μJ and t_{cycle} was measured at 38.9 sec. The obtained end-to-end efficiency is 21%.

V. CONCLUSION

This work presents the design and implementation of a dual band rectifier system with a commodity DC-DC converter. Its high efficiency and tested operation at low-power input could perhaps enable a variety of WSN and Internet-of-Things applications, powered by ambient RF. The circuit was designed with two single diodes, on a low-cost, lossy FR-4 substrate. Also a multi-band antenna was designed and constructed. Experimental results with a commodity DC-DC converter from cold-start were also presented and discussed.

ACKNOWLEDGMENT

This work was supported by the COST Action IC1301 WiPE Wireless Power Transmission for Sustainable Electronics. The work of Christos Kalialakis and Apostolos Georgiadis has been supported by European Unions Horizon 2020 research and innovation programme under the Marie Skłodowska-Curie grant agreements No 654734 and 661621. The authors also would like to thank Coilcraft, Inc. for providing the inductors used in the development of the DC-combining circuit prototype.

REFERENCES

[1] S. Kim, R. Vyas, J. Bito, K. Niotaki, A. Collado, A. Georgiadis, and M. M. Tentzeris, "Ambient RF energy-harvesting technologies for self-sustainable standalone wireless sensor platforms," *Proc. IEEE*, vol. 102, no. 11, pp. 1649–1666, 2014.

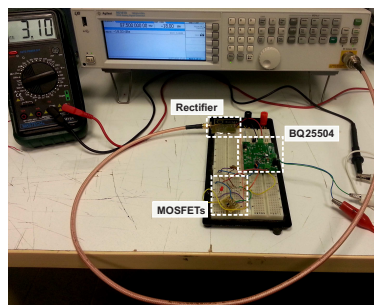


Fig. 13. Measurement setup with rectifier, signal generator, boost converter and MOSFET transistors.

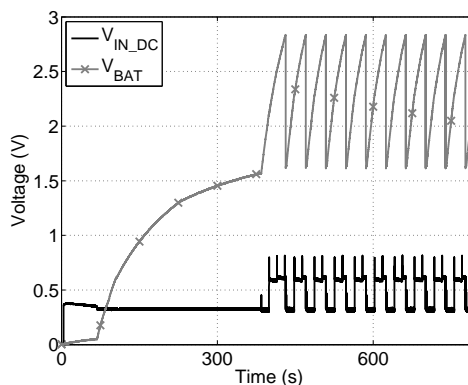


Fig. 14. Boost converter input and output voltage measurement. Voltage across 100 μF capacitor (V_{BAT}), and open circuit voltage across the rectifier output ($V_{\text{IN_DC}}$) for $P_{\text{in}} = -15$ dBm and $F = 97.5$ MHz.

[2] S. Kim, C. Mariotti, F. Alimenti, P. Mezzanotte, A. Georgiadis, A. Collado, L. Roselli, and M. M. Tentzeris, "No battery required: perpetual rfid-enabled wireless sensors for cognitive intelligence applications," *IEEE Microw. Mag.*, vol. 14, no. 5, pp. 66–77, 2013.

[3] S. N. Daskalakis, S. D. Assimonis, E. Kampianakis, and A. Bletsas, "Soil moisture wireless sensing with analog scatter radio, low power, ultra-low cost and extended communication ranges," in *IEEE Sensors Conf.*, 2014, pp. 122–125.

[4] E. Kampianakis, J. Kimionis, K. Tountas, C. Konstantopoulos, E. Koutroulis, and A. Bletsas, "Wireless environmental sensor networking with analog scatter radio and timer principles," *IEEE Sensors J.*, vol. 14, no. 10, pp. 3365–3376, 2014.

[5] J. Kimionis, A. Bletsas, and J. N. Sahalos, "Increased range bistatic scatter radio," *IEEE Trans. Commun.*, vol. 62, no. 3, pp. 1091–1104, 2014.

[6] N. Fasarakis-Hilliard, P. Alevizos, and A. Bletsas, "Coherent detection and channel coding for bistatic scatter radio sensor networking," *IEEE Trans. Commun.*, vol. 63, no. 5, pp. 1798–1810, 2015.

[7] F. Lin, Y.-C. Kuo, J.-W. Hsieh, H.-Y. Tsai, Y. Liao, and H. Lee, "A self-powering wireless environment monitoring system using soil energy," *IEEE Sensors J.*, vol. 15, no. 7, pp. 3751–3758, 2015.

[8] K. Niotaki, F. Giuppi, A. Georgiadis, and A. Collado, "Solar/EM energy harvester for autonomous operation of a monitoring sensor platform," *Wireless Power Transfer*, vol. 1, no. 01, pp. 44–50, 2014.

[9] S. D. Assimonis, S.-N. Daskalakis, and A. Bletsas, "Efficient RF harvesting for low-power input with low-cost lossy substrate rectenna grid," in *IEEE RFID Technology and Applications Conf. (RFID-TA)*, 2014, pp. 1–6.

[10] Texas Instruments, "Ultra low power boost converter with battery management for energy harvester applications," URL: <http://www.ti.com/lit/ds/symlink/bq25504.pdf>, 2011.

[11] M. Piñuela, P. D. Mitcheson, and S. Lucyszyn, "Ambient RF energy harvesting in urban and semi-urban environments," *IEEE Trans. Microw. Theory Techn.*, vol. 61, no. 7, pp. 2715–2726, 2013.